PHYSICAL REVIEW D **94,** 053012 (2016)

Energy spectrum of the electroweak Pomeron

Jochen Bartels,[1] Eugene Levin,[2,3] and Marat Siddikov[3]
[1]*II. Institut für Theoretische Physik, Universität Hamburg, Luruper Chaussee 149, D-22761 Hamburg, Germany*
[2]*Department of Particle Physics, School of Physics and Astronomy, Raymond and Beverly Sackler Faculty of Exact Science, Tel Aviv University, Tel Aviv 69978, Israel*
[3]*Departemento de Física, Universidad Técnica Federico Santa María, Centro Científico-Tecnológico de Valparaíso, Avenida España 1680, Casilla 110-V Valparaíso, Chile*
(Received 6 August 2016; published 27 September 2016)

In this paper we study the high energy behavior of electroweak Standard Model for a nonzero Weinberg angle θ_W. We evaluate the spectrum of the electroweak Pomeron and demonstrate that the leading intercept is given by $\alpha_{\text{e.w.}} 4\ln 2$ and does not depend on the mixing angle θ_W. Due to its very small numerical value, we conclude that the high energy behavior of electroweak theory cannot be discussed without including the QCD Pomeron which, at sufficiently large energies, will dominate.

DOI: 10.1103/PhysRevD.94.053012

I. INTRODUCTION

High energy scattering processes described by the $SU(2) \otimes U(1)$ gauge theory of electroweak interactions, in particular the elastic scattering of weak vector bosons, have played an important role in unravelling the gauge structure of the electroweak sector. From the very beginning the Higgs mechanism was conceived as a way to avoid power law violations of unitarity at high energies. Nevertheless, due to logarithmic loop corrections, resummation is required in order to understand the asymptotic high energy behavior of the theory. In a pure electroweak weak theory these corrections stem from the Reggeization of the electroweak gauge bosons and from the formation of the electroweak Pomeron [1]. When the QCD sector is taken into account, due to formation of virtual quarks, also the QCD Pomeron [2,3] starts contributing [4] and eventually overtakes the electroweak Pomeron. This implies that the unitarization problem in the electroweak sector is still awaiting its final solution.

Due to the rich particle content of the Standard Model, the study of the electroweak Pomeron is a challenging task. As a first step, the decoupled limit ($\theta_w = 0$) of the spectrum of the $SU(2)$ Pomeron was studied in [5,6], and it has been found that the inclusion of a vector meson mass does not affect the spectrum of the Pomerons. However, it does change significantly the form of the eigenfunctions.

In this paper we extend this study to the realistic case of a nonzero mixing angle θ_w. *A priori* it is not clear how mixing might affect the high energy behavior, given the fact that the Higgs mechanism, even in the leading logarithmic approximation, introduces new contributions to the interaction kernels. As a first step, we will work in the leading logarithmic approximation and neglect effects of the running coupling constant. Our main (numerical) result is that the $\theta_w \neq 0$ corrections to the eigenvalue spectrum are small, indicating that the eigenvalues of the electroweak Pomeron coincide with our earlier results [5,6] for an $SU(2)$ gauge theory.

Our paper is organized as follows. In Sec. II we give a short overview of the Balitski-Fadin-Kuraev-Lipatov (BFKL) approach applied to electroweak interactions. First (Sec. II A) we review the case when the Higgs field is absent, then (Sec. II B) we analyze how the Higgs mechanism leads to a system of coupled equations for the electroweak Pomeron [1], and finally (Sec. II C) we demonstrate that the Higgs mechanism does not affect the large-transverse momentum limit of the theory. In order to study the influence of the small-momentum region on the physically important leading intercept, we then perform, in Sec. III, a perturbative expansion in $\sin^2\theta_W$, making use of the smallness of the Weinberg angle. After a short review of our numerical methods developed earlier [5,6] we compute corrections to the leading intercept of the order $\mathcal{O}(\sin^2\theta_W)$ and argue that they vanish. After that in Sec. IV we reduce our system of initially 17 coupled equations for the electroweak Pomeron to a single equation (which is linear in the wave function, but has a complicated dependence on the eigenvaule ω) and perform a numerical analysis in the lattice approximation. Finally, in Sec. V we draw our conclusions.

II. ELECTROWEAK INTERACTIONS AT HIGH ENERGIES: GENERALITIES

A. The massless $SU(2)$ Pomeron

The Lagrangian of the electroweak interaction can be written as a sum of several contributions [7],

$$\mathcal{L}_{\text{EW}} = \mathcal{L}_{\text{gauge}} + \mathcal{L}_{\text{fermions}} + \mathcal{L}_{\text{Higgs boson}} + \mathcal{L}_{\text{Yukawa}}, \quad (1)$$

where $\mathcal{L}_{\text{gauge}}$ has the form

 © 2016 American Physical Society

$$\mathcal{L}_{\text{gauge}} = -\frac{1}{4} W_a^{\mu\nu} W^a_{\mu\nu} - \frac{1}{4} B^{\mu\nu} B_{\mu\nu}, \tag{2}$$

and $W^a_{\mu\nu}$ and $B_{\mu\nu}$ are the field strength tensors for the gauge fields of groups $SU(2)$ and $U(1)$ respectively. For a moment we disregard completely all the other terms in Eq. (1) since at high energy only exchange of the vector gauge fields [8] gives the contributions to the leading $\ln(1/x)$ order of perturbative QCD (LLA).[1] In LLA the massless field W^a_μ Reggeizes and the behavior of the scattering amplitude at high energies is governed by the BFKL evolution [12–14][2]

$$\phi_W(k^2, Y = \ln(1/x)) = \int \frac{d\omega}{2\pi i} e^{\omega Y} \phi_W(\omega, k^2), \tag{3}$$

where

$$\omega \phi_W(\omega, k^2) = \bar{\alpha}_{\text{e.w.}} \left\{ \int \frac{dk'^2}{|k^2 - k'^2| + k\epsilon} \phi_W(\omega, k'^2) - \ln(k^2/\epsilon^2) \phi_W(\omega, k^2) \right\}, \tag{4}$$

$\bar{\alpha}_{\text{e.w.}} = \frac{g^2}{4\pi} \frac{2}{\pi}$ for the $SU(2)$ group, the second term in (4) stems from vector boson Reggeization, and $\epsilon \to 0$ provides a regularization near the point $k^2 = k'^2$ in the emission kernel. The solution of (4) is well known [8,9]. The eigenvalues (spectrum) of the BFKL equation is continuous and is parametrized by a variable ν which is related to the eigenvalue as

$$\omega_{\text{e.w.BFKL}}(\nu) = \bar{\alpha}_{\text{e.w.}} \left(2\psi(1) - \psi\left(\frac{1}{2} - i\nu\right) - \psi\left(\frac{1}{2} + i\nu\right) \right), \tag{5}$$

where $\psi(z)$ is a polygamma function. The spectrum (5) is limited from above by $\omega(\nu = 0) = 4 \ln 2 \bar{\alpha}_{\text{e.w.}}$, which yields for the large-s behavior $s^{1+\omega(\nu=0)}$. For all other ν, the spectrum is twice degenerate, with eigenfunctions given by

$$\phi_W^{\text{BFKL}}(k^2) = (k^2)^{-\frac{1}{2} \pm i\nu}. \tag{6}$$

The set (6) forms an orthonormalized and a complete set of functions. The Abelian fields B_ν do not interact with each other in LLA and they lead to the amplitude which is proportional to s [10].

B. Symmetry breaking and the electroweak Pomeron

As peculiar features of the electroweak theory, due to a Higgs mechanism gauge bosons get masses (which, naively speaking, we expect not to affect high energy behavior of a theory) and physical fields Z and γ are defined as mixtures of gauge fields W^3 and B. Taking into account that only W^3 Reggeizes, it is not clear how the switch from (W^3, B) to physical (Z, γ) will affect a high energy behavior of the theory. For this reason it is not obvious: on the one hand, we expect that a low-energy spontaneous symmetry breaking cannot affect the high energy amplitudes. On the other hand, the Higgs field couples to both gauge fields and generates new vertices absent in unbroken theory. The systematic investigation of high energy scattering in the electroweak sector in the leading log approximation was described in [1]. It was found that the charged gauge bosons Reggeizes, and the corresponding trajectory function is given by

$$\omega_c(t) = \alpha_c(t) - 1 = (t - M_W^2)(c_W^2 \beta_{WZ}(t) + s_W^2 \beta_{W\gamma}(t)), \tag{7}$$

where $c_W \equiv \cos\theta_W$, $s_W \equiv \sin\theta_W$, $t = -q^2$, q is a transverse momentum of a boson, and

$$\beta_{ij}(t) = \frac{\bar{\alpha}_{ew}}{4\pi} \int d^2k \frac{1}{k^2 + M_i^2} \frac{1}{(k-q)^2 + M_j^2}. \tag{8}$$

In a neutral channel, the situation is more complicated since Reggeization exists for a linear combination of Z-boson and photon γ which corresponds to a component W^3 of the $SU(2)$ gauge field. A general consideration in this case is complicated, and it was demonstrated in [1] that it can be significantly simplified if we consider this Reggeizeable part as a separate contribution of two auxiliary fictitious fields n and 3, assuming that Z and γ do not Reggeize at all. The corresponding propagators of real and fictitious particles are given by

$$Z \to \frac{c_W^2}{\omega} \frac{1}{q^2 + M_Z^2}, \qquad \gamma \to \frac{s_W^2}{\omega} \frac{1}{q^2},$$
$$n \to \frac{1}{\omega - \omega_n(q^2)} \frac{1}{q^2 + M_W^2} 3 \to -\frac{1}{\omega} \frac{1}{q^2 + M_W^2}, \tag{9}$$

and the neutral trajectory is defined as

$$\omega_n(t) = \alpha_n(t) - 1 = (t - M_W^2) \beta_{WW}(t), \tag{10}$$

where β_{WW} is given by (8). The trajectory function $\alpha_n(t)$ passes though unity at $t = M_W^2$, i.e. neither the Z-boson nor

[1] In LLA we sum all Feynman diagrams considering $\bar{\alpha}_S \ll 1, \bar{\alpha}_S \ln(1/x) \sim 1$ and $\bar{\alpha}_S \ln(Q^2) \ll 1$.

[2] Throughout this paper, we will be interested in the BFKL eigenvalue problem. Rather than dealing with BFKL-Green's functions, $G_\omega(q, k, k')$, we therefore define amplitudes by convoluting the Green's function at one end with some impact factor (which we do not need to specify). The resulting amplitudes $\phi(\omega, q, k)$ are defined to include one of the external momentum propagators.

the photon lie on this trajectory. In the limit $\theta_W \to 0$ the sum of the four exchanges (9) reduces to

$$\frac{1}{\omega-\omega_n(t)}\frac{1}{q^2+M_W^2}, \tag{11}$$

and ω_c and ω_n coincide. For large momenta only the contribution of the field n survives,

$$\frac{c_W^2}{q^2+M_Z^2}+\frac{s_W^2}{q^2}-\frac{1}{q^2+M_W^2}=\mathcal{O}\left(\frac{M_W^4}{(q^2)^3}\right). \tag{12}$$

When formulating coupled integral equations for the different exchange channels, it was found to be convenient to treat the four terms in (9) as independent states: $Z,\gamma,n,3$. In the following we will use the bracketed notations $\{Zn\}=Zn+nZ$ and $\{n3\}=3n+n3$.

The corresponding eigenfunctions of BFKL evolution should satisfy a system of coupled equations[3]

$$(\omega-\omega_i(k)-\omega_j(k))\Phi_{ij}(k) = \int\frac{d^2k'}{(2\pi)^3}\sum_{i'j'\neq\gamma}K_{ij,j'j'}\frac{(-1)^{N_3(i',j')}c_W^{2N_Z(i',j')}\Phi_{i'j'}(k')}{D(k',M_i)D(k',M_j)} \tag{13}$$

$$+\sqrt{2}\int\frac{d^2k''}{(2\pi)^3}K_{ij,cc}(k,k')\frac{\Phi_{cc}(k')}{D(k',M_W)^2} \tag{14}$$

$$(\omega-2\omega_c(k))\Phi_{cc}(k) = \sqrt{2}\int\frac{d^2k'}{(2\pi)^3} \times\sum_{i'j'}K_{cc,ij}\frac{(-1)^{N_3(i,j)}c_W^{2N_Z(i,j)}s_W^{2N_\gamma(i,j)}\Phi_{ij}(k')}{D(k',M_i)D(k',M_j)} \tag{15}$$

$$+\int\frac{d^2k'}{(2\pi)^3}K_{cc,cc}(k,k')\frac{\Phi_{cc}(k')}{D(k',M_W)^2}, \tag{16}$$

where indices i,j,i',j', unless stated otherwise, run over above-mentioned neutral states $Z,\gamma,n,3$; and $N_m(i,j)$ stands for the number of times "m" appears among its arguments [so for example $N_Z(Z,Z)=2$, $N_Z(Z,\gamma)=1,\ldots$]. The factors $(-1)^{N_3(i,j)}c_W^{2N_Z(i,j)}s_W^{2N_\gamma(i,j)}$ appear from numerators of propagators, and in denominators which stem from propagators (9) we use shorthand notations $D(k,M_i)\equiv k^2+M_i^2$. For the sake of brevity we will use an abbreviation $D(k)\equiv D(k,M_W)$, and $M_W\equiv M$. The corresponding kernels have a form

$$K_{ij,j'j'}=\frac{g^2M_W^2}{2c_W^{2N_Z(i,j,i',j')}}\theta(i,j,i',j'\neq\gamma), \tag{17}$$

$$K_{ij,cc}(k,k') = g^2\left(-M_{ij}^2+\frac{(D(k,M_i)+D(k,M_j))D(k')}{D(k-k')}\right) = g^2\left(-M_{ij}^2+2K_{em}(k,k') +\frac{(M_i^2+M_j^2-2M_W^2)D(k')}{D(k-k')}\right), \tag{18}$$

$$K_{em}(k,k')=g^2\frac{D(k)D(k')}{D(k-k')}=g^2K_{em}(k,k',M_W), \tag{19}$$

$$K_{em}(k,k',M)=g^2\frac{D(k)D(k')}{D(k-k',M)}, \tag{20}$$

$$M_{ij}^2=M_i^2+M_j^2-\frac{M_i^2M_j^2}{2M_W^2}, \tag{21}$$

$$K_{cc,cc} = g^2\left(-M_W^2+D(k)D(k') \times\left(\frac{c_W^2}{D(k-k',M_Z)}+\frac{s_W^2}{D(k-k',0)}\right)\right) \equiv g^2(-M_W^2+(c_W^2K_{em}(k,k',M_Z) +s_W^2K_{em}(k,k',M_Z))), \tag{22}$$

where the θ-function in (17) reflects the fact that the kernel $K_{ij,i'j'}$ vanishes if any of the indices is γ.[4] In these notations the trajectories (7) and (10) can be rewritten as

$$\omega_i(k)=-\delta_{i,n}g^2\int\frac{d^2k'}{(2\pi)^3}\frac{D(k)}{D(k')D(k-k')}, \tag{23}$$

$$\omega_c(k) = -g^2\int\frac{d^2k'}{(2\pi)^3}\frac{D(k)}{D(k')} \times\left(\frac{c_W^2}{D(k-k',M_Z)}+\frac{s_W^2}{D(k-k',0)}\right). \tag{24}$$

C. Large momentum asymptotics

At large transverse momenta $k\gg M$, we expect that the theory should not depend on a value of mixing angle θ_W. We will show explicitly that in this region the system of equations reduces to the equation for the $SU(2)$ Pomeron, supporting the intuitive expectation that the low-energy symmetry breaking does not affect the high energy asymptotic behavior of the scattering amplitude. In the region of

[3]For simplicity in this paper we restrict ourselves to the forward region $q=0$.

[4]This happens because in the leading order over α_{EW} there are no terms with a direct coupling of a Higgs boson to a massless photon.

large transverse momenta $k, k', |k-k'| \gg M$ we can neglect all the masses, so the emission kernels take a form

$$K_{ij,cc}(k,k') \approx 2g^2 K^{\mathrm{BFKL}}(k,k'), \tag{25}$$

$$K_{cc,cc} \approx g^2 K^{\mathrm{BFKL}}(k,k'), \tag{26}$$

where the BFKL kernel is given by

$$K^{\mathrm{BFKL}}(k,k') = g^2 \frac{k^2 k'^2}{(k-k')^2}. \tag{27}$$

Equation (13) simplifies to

$$(\omega - \omega_i(k) - \omega_j(k))\Phi_{ij}(k) \approx 2\sqrt{2}g^2 \int \frac{d^2k'}{(2\pi)^3} \frac{K^{\mathrm{BFKL}}(k,k')}{D(k',M_W)^2} \Phi_{cc}(k') \tag{28}$$

and implies that neutral fields Φ_{ij} differ only due to Regge trajectories in the lhs of (28). In particular, using (23) and (24), we may get that at large momenta

$$\Phi_{ZZ} \approx \Phi_{\gamma\gamma} \approx \Phi_{33} \approx \Phi_{Z\gamma} \approx \Phi_{Z3} \approx \Phi_{\gamma 3}, \tag{29}$$

$$\Phi_{Zn} \approx \Phi_{3n} \approx \Phi_{Z3}. \tag{30}$$

Combining this with (12), we can see that in (12) the contribution of all components with indices Z, γ or 3 mutually cancel (decouple) at large k, i.e. in (15) only a field "n" contributes. Also, we can notice that there are no terms which depend explicitly on θ_W. If we assume that $\sqrt{2}\Phi_{nn}(k) = \Phi_{cc}$ and does not depend on azimuthal angle, after redefinition

$$\phi_W^{\mathrm{BFKL}}(k) = \frac{\Phi_{cc}(k)}{D(k,M)} \tag{31}$$

we may reproduce (4). It is known that the large-k asymptotics of solutions of (4) are the same as in massive case (6),

$$\phi_{ij}^{\mathrm{BFKL}}(k) \propto (k^2)^{-\frac{1}{2}\pm i\nu}, \tag{32}$$

such that

$$\Phi_{ij}(k) \propto (k^2)^{\frac{1}{2}\pm i\nu}. \tag{33}$$

The fact that $\Phi_{ij}(k)$ grows at large k justifies omission of contact terms in (13) and finalizes our proof that for asymptotically large k the eigenfunctions and eigenvalues coincide with the $SU(2)$ Pomeron, independently of the value of θ_W.

A crucial assumption which was implicitly used in this section is that if we consider large momentum k, then in the integrals in (13) and (15) the dominant contribution also comes from large k' and large $|k-k'|$. Potentially the latter assumption might be violated near $k \approx k'$, where the emission kernel (19) is strongly peaked, giving rise to a strong sensitivity to θ_W. For this reason in the following Sec. III we perform an analysis of $\mathcal{O}(\theta_w)$ corrections and demonstrate explicitly that it does not affect the spectrum. Additionally, the proof given above could be invalidated by localized solutions which fall off rapidly at large k as $\phi_{i,j} \propto 1/k^2$ or faster (see Appendix A 1 for a particular example of such a solution). If such solutions exist and have intercept $\omega > \omega^{\mathrm{BFKL}}(\nu = 0)$, potentially they could significantly change the evolution of the BFKL spectrum. For this reason in Sec. IV we perform a general analysis in the lattice and demonstrate that there are no such solutions.

III. PERTURBATIVE ANALYSIS IN THE SMALL-θ_W LIMIT

In this section we develop a systematic perturbative expansion of (13) and (15) over the parameter $s_w^2 = \sin^2\theta_W$ up to the first order of perturbation theory. In addition to explicit dependence on the Weinberg angle in (9). we should also take into account the θ_w dependence in Z-boson mass,

$$M_Z^2 = \frac{M_W^2}{c_W^2} \approx M_W^2(1+s_w^2). \tag{34}$$

The trajectory $\omega_c(q^2)$ in this limit may be expanded as

$$\omega_c(q^2) \approx \omega_n(q^2) + s_W^2 \Delta\omega_c(q^2), \tag{35}$$

where

$$\Delta\omega_c(q^2) = \bar{\alpha}_{ew}(q^2 - M^2) \int \frac{d^2k}{4\pi} \frac{M^4}{k^2 D(k)^2 D(q-k)}. \tag{36}$$

From now on we use a notation Δ for the corrections proportional to s_w^2. The kernel $K_{ij,i'j'}$ given in (17) may be expanded as

$$K_{ij,i'j'} \approx \frac{g^2 M_W^2}{2} \theta(i,j,i',j' \neq \gamma)(1 + N_Z(i,j,i',j')s_W^2). \tag{37}$$

In a similar fashion, using the expansion of M_{ij}^2,

$$\begin{aligned} M_{ZZ}^2 &= \frac{3}{2}M^2 + s_w^2 M^2 \\ M_{Z\gamma}^2 &= M^2 + s_w^2 M^2 \\ M_{Zn}^2 &= \frac{3}{2}M^2 + \frac{1}{2}s_w^2 M^2. \end{aligned} \tag{38}$$

$$M^2_{\gamma\gamma} = 0$$
$$M^2_{nn} = \frac{3}{2}M^2$$
$$M^2_{\gamma n} = M^2$$
$$M^2_{n\gamma} = M^2, \tag{39}$$

we may obtain for the kernels with account of $\mathcal{O}(s_w^2)$ corrections

$$K_{ZZ;cc} = g^2\left(\left(-q^2 - \frac{3}{2}M^2\right) + \frac{D(k)D(q-k') + D(q-k)D(k')}{D(k-k')}\right) + s_w^2 g^2\left(-M^2 + M^2\frac{D(k) + D(q-k)}{D(k-k')}\right) \tag{40}$$

$$K_{Z\gamma;cc} = g^2\left(-q^2 - M^2 + \frac{D(k)D(q-k') + (q-k)^2 D(k')}{D(k-k')}\right) + s_w^2 g^2\left(-M^2 + M^2\frac{D(q-k')}{D(k-k')}\right) \tag{41}$$

$$K_{\gamma Z;cc} = g^2\left(-q^2 - M^2 + \frac{k^2 D(q-k') + D(q-k)D(k')}{D(k-k')}\right) + s_w^2 g^2\left(-M^2 + M^2\frac{D(k')}{D(k-k')}\right) \tag{42}$$

$$K_{Zn;cc} = g^2\left(-q^2 - \frac{3}{2}M^2 + \frac{D(k)D(q-k') + D(q-k)D(k')}{D(k-k')}\right) + s_w^2 g^2\left(-\frac{M^2}{2} + M^2\frac{D(q-k')}{D(k-k')}\right) \tag{43}$$

$$K_{nZ;cc} = g^2\left(-q^2 - \frac{3}{2}M^2 + \frac{D(k)D(q-k') + D(q-k)D(k')}{D(k-k')}\right) + s_w^2 g^2\left(-\frac{M^2}{2} + M^2\frac{D(k')}{D(k-k')}\right) \tag{44}$$

$$K_{\gamma\gamma;cc} = g^2\left(-q^2 + \frac{k^2 D(q-k') + (q-k)^2 D(k')}{D(k-k')}\right) \tag{45}$$

$$K_{\gamma n;cc} = g^2\left(-q^2 - M^2 + \frac{k^2 D(q-k') + D(q-k)D(k')}{D(k-k')}\right) \tag{46}$$

$$K_{n\gamma;cc} = g^2\left(-q^2 - M^2 + \frac{D(k)D(q-k') + (q-k)^2 D(k')}{D(k-k')}\right) \tag{47}$$

$$K_{nn;cc} = g^2\left(-q^2 - \frac{3}{2}M^2 + \frac{D(k)D(q-k') + D(q-k)D(k')}{D(k-k')}\right) \tag{48}$$

$$K_{cc;ij}(q,k,k') = K_{ij;cc}(q,k',k). \tag{49}$$

$$K_{cc;cc} = g^2\left(-q^2 - M^2 + \frac{D(k)D(q-k') + D(q-k)D(k')}{D(k-k')}\right) + s_w^2 g^2 M^4 \frac{D(k)D(q-k') + D(q-k)D(k')}{(k-k')^2 D(k-k')^2}. \tag{50}$$

In what follows it is convenient to introduce a shorthand notation $\Delta\mathcal{K}$ for all $\mathcal{O}(s_W^2)$-corrections, both due to kernels and propagators. In the case of a $\Delta\mathcal{K}_{cc;cc}$ component, we should also add an $\mathcal{O}(s_W^2)$-contribution from the Regge trajectory,

$$\Delta\mathcal{K}_{cc;cc} = (\Delta K_{cc;cc} + (\Delta\omega(-k^2) + \Delta\omega(-(q-k)^2)) \times \delta^{(2)}(k-k'))\frac{1}{D(k')D(q-k')}, \tag{51}$$

and it is straightforward to verify that there is a cancellation of the s-channel photon pole. The other components of operator $\Delta\mathcal{K}$ are given explicitly as

$$\Delta\mathcal{K}_{\gamma\gamma,cc} = 0, \qquad \Delta\mathcal{K}_{nn,cc} = 0, \qquad \Delta\mathcal{K}_{\gamma n,cc} = 0 \tag{52}$$

$$\Delta\mathcal{K}_{cc;\gamma n} = \Delta\mathcal{K}_{cc;\gamma Z}, \qquad \Delta\mathcal{K}_{cc;n\gamma} = \Delta\mathcal{K}_{cc;Z\gamma} \tag{53}$$

$$\Delta\mathcal{K}_{cc;ZZ} = g^2\left(2(q^2 + M^2) + \left(q^2 + \frac{3}{2}M^2\right) \times \left[\frac{M^2}{D(k')} + \frac{M^2}{D(q-k')}\right] - \frac{M^2}{D(k-k')} \times \left[\frac{D(k)}{D(k')}D(q-k') + \frac{D(q-k)}{D(q-k')}D(k')\right] - 2\frac{D(k)D(q-k') + D(q-k)D(k')}{D(k-k')}\right) \times \frac{1}{D(k')D(q-k')} \tag{54}$$

$$\Delta K_{cc;Zn} = g^2\left(q^2 + M^2 + \left(q^2 + \frac{3}{2}M^2\right)\frac{M^2}{D(k')} + \frac{M^2}{D(k-k')}\left[D(k) - \frac{D(k)}{D(k')}D(q-k')\right] - \frac{D(k)D(q-k') + D(q-k)D(k')}{D(k-k')}\right) \times \frac{1}{D(k')D(q-k')} \tag{55}$$

$$\Delta\mathcal{K}_{cc;nZ} = g^2\left(q^2+M^2+\left(q^2+\frac{3}{2}M^2\right)\frac{M^2}{D(q-k')} + \frac{M^2}{D(k-k')}\left[D(q-k)-\frac{D(q-k)}{D(q-k')}D(k')\right] - \frac{D(k)D(q-k')+D(q-k)D(k')}{D(k-k')}\right) \times \frac{1}{D(k')D(q-k')} \tag{56}$$

$$\Delta\mathcal{K}_{cc;\gamma Z} = g^2\left(-q^2-M^2+\frac{D(k)D(q-k')+D(q-k)k'^2}{D(k-k')}\right) \times \frac{1}{k'^2 D(q-k')} \tag{57}$$

$$\Delta\mathcal{K}_{cc;Z\gamma} = g^2\left(-q^2-M^2+\frac{D(k)(q-k')^2+D(q-k)D(k')}{D(k-k')}\right) \times \frac{1}{D(k')(q-k')^2}. \tag{58}$$

Finally the transitions neutral → neutral. Here we have corrections both from the kernels and from the propagators of the Z-boson and of the photon. There are no corrections from the trajectory functions, so they only contribute to the leading order diagonal kernels $nn \to nn$. In the following we list the corrections for the different channels:

$$\Delta\mathcal{K}_{ZZ;ZZ} = g^2\frac{M^2}{2}\left(2-\frac{M^2}{D(k')}-\frac{M^2}{D(q-k')}\right)\frac{1}{D(k')D(q-k')} \tag{59}$$

$$\Delta\mathcal{K}_{nZ;ZZ} = g^2\frac{M^2}{2}\left(1-\frac{M^2}{D(k')}-\frac{M^2}{D(q-k')}\right)\frac{1}{D(k')D(q-k')} \tag{60}$$

$$\Delta\mathcal{K}_{nn;ZZ} = g^2\frac{M^2}{2}\left(-\frac{M^2}{D(k')}-\frac{M^2}{D(q-k')}\right)\frac{1}{D(k')D(q-k')} \tag{61}$$

$$\Delta\mathcal{K}_{ZZ;Zn} = g^2\frac{M^2}{2}\left(2-\frac{M^2}{D(k')}\right)\frac{1}{D(k')D(q-k')} \tag{62}$$

$$\Delta\mathcal{K}_{nZ;Zn} = g^2\frac{M^2}{2}\left(1-\frac{M^2}{D(k')}\right)\frac{1}{D(k')D(q-k')} \tag{63}$$

$$\Delta\mathcal{K}_{nn;Zn} = g^2\frac{M^2}{2}\left(-\frac{M^2}{D(k')}\right)\frac{1}{D(k')D(q-k')} \tag{64}$$

$$\Delta\mathcal{K}_{ZZ;nn} = 2g^2\frac{M^2}{2} \tag{65}$$

$$\Delta\mathcal{K}_{Zn;nn} = g^2\frac{M^2}{2}. \tag{66}$$

The remaining kernels are easily obtained using a symmetry $\Delta K_{ij,i'j'} = \Delta K_{ji,i'j'} = \Delta K_{ij,j'i'}$.

A. The case of zero Weinberg angle, $\theta_W = 0$

In this section we study the eigenvalues for the case $\theta_W = 0$. In this limit the set of equations (13) and (15) simplifies considerably, since the photon field decouples from the other equations, and the other neutral fields have the same mass. Besides, all the kernels K no longer distinguish these states, and the only differences among the neutral states is due to the nonzero Regge trajectory of n. In this limit the system (13) and (15) reduces to a system of seven coupled equations:

$$\omega\Phi_{ZZ}(k) = \frac{g^2}{2}\int\frac{d^2k'}{(2\pi)^3}\frac{1}{D^2(k')}\left(\sum_{ij\neq\gamma}(-1)^{N_3}\Phi_{ij}(k')-3\sqrt{2}\Phi_{cc}(k')\right)+2\sqrt{2}\int\frac{d^2k'}{(2\pi)^3}\frac{1}{D^2(k')}K_{em}(k,k')\Phi_{cc}(k'), \tag{67}$$

$$(\omega-\omega_n(k))\Phi_{Zn}(k) = \frac{g^2}{2}\int\frac{d^2k'}{(2\pi)^3}\frac{1}{D^2(k')}\left(\sum_{ij\neq\gamma}(-1)^{N_3}\Phi_{ij}(k')-3\sqrt{2}\Phi_{cc}(k')\right)+2\sqrt{2}\int\frac{d^2k'}{(2\pi)^3}\frac{1}{D^2(k')}K_{em}(k,k')\Phi_{cc}(k'), \tag{68}$$

$$\omega\Phi_{Z3}(k) = \frac{g^2}{2}\int\frac{d^2k'}{(2\pi)^3}\frac{1}{D^2(k')}\left(\sum_{ij\neq\gamma}(-1)^{N_3}\Phi_{ij}(k')-3\sqrt{2}\Phi_{cc}(k')\right)+2\sqrt{2}\int\frac{d^2k'}{(2\pi)^3}\frac{1}{D^2(k')}K_{em}(k,k')\Phi_{cc}(k'), \tag{69}$$

$$\omega\Phi_{33}(k) = \frac{g^2}{2}\int \frac{d^2k'}{(2\pi)^3}\frac{1}{D^2(k')}\left(\sum_{ij\neq\gamma}(-1)^{N_3}\Phi_{ij}(k') - 3\sqrt{2}\Phi_{cc}(k')\right) + 2\sqrt{2}\int \frac{d^2k'}{(2\pi)^3}\frac{1}{D^2(k')}K_{em}(k,k')\Phi_{cc}(k'), \tag{70}$$

$$(\omega-\omega_n(k))\Phi_{n3}(k) = \frac{g^2}{2}\int \frac{d^2k'}{(2\pi)^3}\frac{1}{D^2(k')}\left(\sum_{ij\neq\gamma}(-1)^{N_3}\Phi_{ij}(k') - 3\sqrt{2}\Phi_{cc}(k')\right) + 2\sqrt{2}\int \frac{d^2k'}{(2\pi)^3}\frac{1}{D^2(k')}K_{em}(k,k')\Phi_{cc}(k'), \tag{71}$$

$$(\omega-2\omega_n(k))\Phi_{nn}(k) = \frac{g^2}{2}\int \frac{d^2k'}{(2\pi)^3}\frac{1}{D^2(k')}\left(\sum_{ij\neq\gamma}(-1)^{N_3}\Phi_{ij}(k') - 3\sqrt{2}\Phi_{cc}(k')\right) + 2\sqrt{2}\int \frac{d^2k'}{(2\pi)^3}\frac{1}{D^2(k')}K_{em}(k,k')\Phi_{cc}(k'), \tag{72}$$

$$\begin{aligned}(\omega-2\omega_n(k))\Phi_{cc}(k) = {}& -g^2\int \frac{d^2k'}{(2\pi)^3}\frac{1}{D^2(k')}\left(\frac{3\sqrt{2}}{2}\sum_{ij\neq\gamma}(-1)^{N_3}\Phi_{ij}(k') + \Phi_{cc}(k')\right)\\ &+ 2\sqrt{2}\int \frac{d^2k'}{(2\pi)^3}\frac{1}{D^2(k')}K_{em}(k,k')\sum_{n_in_j\neq\gamma}(-1)^{N_3}\Phi_{ij}(k') + 2\int \frac{d^2k'}{(2\pi)^3}\frac{1}{D^2(k')}K_{em}(k,k')\Phi_{cc}(k').\end{aligned} \tag{73}$$

There are three more decoupled equations containing a photon:

$$\begin{aligned}(\omega-\omega_n(k))\Phi_{n\gamma}(k) &= -g^2\sqrt{2}\int \frac{d^2k'}{(2\pi)^3}\frac{1}{D^2(k')}\Phi_{cc}(k') + 2\sqrt{2}\int \frac{d^2k'}{(2\pi)^3}\frac{1}{D^2(k')}K_{em}(k,k')\Phi_{cc}(k'),\\ \omega\Phi_{Z\gamma}(k) &= -g^2\sqrt{2}\int \frac{d^2k'}{(2\pi)^3}\frac{1}{D^2(k')}\Phi_{cc}(k') + 2\sqrt{2}\int \frac{d^2k'}{(2\pi)^3}\frac{1}{D^2(k')}K_{em}(k,k')\Phi_{cc}(k'),\\ \omega\Phi_{3\gamma}(k) &= -g^2\sqrt{2}\int \frac{d^2k'}{(2\pi)^3}\frac{1}{D^2(k')}\Phi_{cc}(k') + 2\sqrt{2}\int \frac{d^2k'}{(2\pi)^3}\frac{1}{D^2(k')}K_{em}(k,k')\Phi_{cc}(k'),\end{aligned} \tag{74}$$

$$\omega\Phi_{\gamma\gamma}(k) = 2\sqrt{2}\int \frac{d^2k'}{(2\pi)^3}\frac{1}{D^2(k')}K_{em}(k,k')\Phi_{cc}(k'). \tag{75}$$

As we can see from (67)–(73), there are several coinciding components of Φ_{ij} which we denote as[5]

$$\Phi_{ZZ}(k) = \Phi_{Z3}(k) = \Phi_{33}(k) = \Phi_1(k) \tag{76}$$

$$\Phi_{Zn}(k) = \Phi_{n3}(k) = \frac{\omega}{\omega-\omega_n(k)}\Phi_1(k). \tag{77}$$

Using (76) and (77), the sum over neutral fields in (67)–(73) reduces to

$$\sum_{ij\neq\gamma}(-1)^{N_3}\Phi_{ij}(k') = \Phi_{nn}(k'), \tag{78}$$

and the full system (76) and (77) reduces to a simple system of just two coupled equations. With the substitutions (after the angular integration)

$$g^2\frac{d^2k'}{(2\pi)^3} \to g^2\frac{d\kappa}{8\pi^2} \to \frac{g^2}{4\pi}\frac{d\kappa}{2\pi} = \frac{\bar{\alpha}_{\text{e.w.}}}{4}d\kappa \tag{79}$$

we find

$$\begin{aligned}(\omega-2\omega(k))\Phi_{nn}(k) = {}& \frac{g^2}{2}\int \frac{d^2k'}{(2\pi)^3}\frac{1}{D^2(k')}\\ &\times(\Phi_{nn}(k') - 3\sqrt{2}\Phi_{cc}(k'))\\ &+ 2\sqrt{2}\int \frac{d^2k'}{(2\pi)^3}\frac{K_{em}(k,k')\Phi_{cc}(k')}{D^2(k')},\end{aligned} \tag{80}$$

[5]In contrast to a result found in [1], we can see that not all neutral fields in (76) and (77) coincide due to nonzero Regge trajectory $\omega_n(k)$. In the limit $\theta_W = 0$ this does not affect the eigenvalues, but for the $\mathcal{O}(s_W^2)$ corrections this difference is important.

$$(\omega - 2\omega(k))\Phi_{cc}(k) = -g^2 \int \frac{d^2k'}{(2\pi)^3}\frac{1}{D^2(k')} \times \left(\frac{3\sqrt{2}}{2}\Phi_{nn}(\kappa') + \Phi_{cc}(\kappa')\right) + 2\sqrt{2}g^2 \int \frac{d^2k'}{(2\pi)^3}\frac{K_{em}(k,k')\Phi_{nn}(k')}{D^2(k')} + 2g^2 \int \frac{d^2k'}{(2\pi)^3}\frac{K_{em}(k,k')\Phi_{cc}(k')}{D^2(k')}. \quad (81)$$

As it was discussed in [1], this system of equations (80) and (81) has two solutions, with isospin zero and two. Since we are mostly interested in the leading intercept, in what follows, we will consider only the isospin zero case, for which a solution has a form

$$\begin{pmatrix}\Phi_{nn}(k)\\ \Phi_{cc}(k)\end{pmatrix} = \begin{pmatrix}1\\ \sqrt{2}\end{pmatrix}\Phi(k). \quad (82)$$

We thus end up with a $SU(2)$ BFKL equation for $\Phi(k)$:

$$(\omega - 2\omega(k))\Phi(k) = -g^2\frac{5M_W^2}{2}\int \frac{d^2k'}{(2\pi)^3}\frac{\Phi(k')}{D^2(k')} + 4\int \frac{d^2k'}{(2\pi)^3}\frac{K_{em}(k,k')\Phi(k')}{D^2(k')}, \quad (83)$$

which up to a renormalization of the field Φ coincides with (4) which has been analyzed in detail in [5]. The field Φ_1 defined in (76) is related to Φ as

$$\Phi_1(k) = \frac{\omega - 2\omega(k)}{\omega}\Phi(k) = \left(1 - \frac{2\omega(k)}{\omega}\right)\Phi(k), \quad (84)$$

and for the states with photons we may cast our result into the form

$$\Phi_{n\gamma}(k) = \frac{\omega - 2\omega(k)}{\omega - \omega(k)}\Phi(k) + \frac{g^2}{2(\omega - \omega(k))}\int \frac{d^2k'}{(2\pi)^3}\frac{\Phi(k')}{D^2(k')} \quad (85)$$

$$\Phi_{Z\gamma}(k) = \Phi_{3\gamma}(k) = \frac{\omega - 2\omega(\kappa)}{\omega}\Phi(k) + \frac{g^2}{2\omega}\int \frac{d^2k'}{(2\pi)^3}\frac{\Phi(k')}{D^2(k')} \quad (86)$$

$$\Phi_{\gamma\gamma}(k) = \frac{\omega - 2\omega(\kappa)}{\omega}\Phi(k) + \frac{5g^2}{2\omega}\int \frac{d^2k'}{(2\pi)^3}\frac{\Phi(k')}{D^2(k')}. \quad (87)$$

B. Lattice solutions of the equations for $\theta_W = 0$

1. The method

In this section we analyze the solutions in the lattice using the approach of [6]. Since the solution Φ of (83) at large momenta is growing as (33), it is more convenient to change a normalization as in (31) and will work with a field ϕ which is decreasing at large momenta. Since we are interested only in solutions which do not depend explicitly on azimuthal angle, it is convenient to perform the angular integrations and to introduce the dimensionless variables $\kappa = k^2/M_W^2$ and $\kappa' = k'^2/M_W^2$. Such transition in the integrals in (83) reduces to the substitution (79). The kernel $K_{em}(k,k')$ after angular averaging becomes

$$K_0(\kappa,\kappa') = g^2\frac{(\kappa+1)(\kappa'+1)}{\sqrt{(\kappa-\kappa')^2 + 2(\kappa+\kappa') + 1}}, \quad (88)$$

and Eq. (83) simplifies to

$$\omega\phi(\kappa) = \int d\kappa' K(\kappa,\kappa')\phi(\kappa'), \quad (89)$$

where

$$K(\kappa,\kappa') = \bar{\alpha}_{\text{e.w.}}\left(\frac{1}{\sqrt{(\kappa-\kappa')^2 + 2(\kappa+\kappa') + 1}} - \underbrace{\frac{5}{2}\frac{1}{\kappa+1}\frac{1}{\kappa'+1}}_{\text{contact term}} - \frac{\kappa+1}{\sqrt{\kappa}\sqrt{\kappa+4}}\ln\frac{\sqrt{\kappa+4}+\sqrt{\kappa}}{\sqrt{\kappa+4}-\sqrt{\kappa}}\delta(\kappa-\kappa')\right). \quad (90)$$

For our numerical studies we use a logarithmic grid in both variables κ and κ' with $N+1$ nodes,

$$\kappa_n = \kappa_{\min}\exp\left(\frac{n}{N}\ln(\kappa_{\max}/\kappa_{\min})\right), \quad n = 0,\ldots,N, \quad (91)$$

where the values of $\kappa_{\min}$, $\kappa_{\max}$ were set to $\kappa_{\min} = 10^{-40}$, $\kappa_{\max} = 10^{80}$, and $N = 1024$. In this grid (89) takes a form of linear matrix eigenvalue problem:

$$\omega\phi_n = \sum_{m=0}^{N}\mathcal{K}_{nm}\phi_m, \quad (92)$$

$$\phi_n \equiv \phi(\kappa_n), \quad (93)$$

$$\mathcal{K}_{nm} \equiv K(\kappa_n,\kappa_m)\kappa_m\left(\frac{1}{N}(\kappa_{\max}/\kappa_{\min})\right). \quad (94)$$

In Ref. [5] we solved (92) both for the massive (83) and for the massless BFKL equation. For the latter case the

TABLE I. The first twenty roots of the massive BFKL equation (83).

Root No.	$\omega_n/\bar{\alpha}_{\text{e.w.}}$	Root No.	$\omega_n/\bar{\alpha}_{\text{e.w.}}$	Root No.	$\omega_n/\bar{\alpha}_{\text{e.w.}}$	Root No.	$\omega_n/\bar{\alpha}_{\text{e.w.}}$
1	2.77	6	2.61	11	2.27	16	1.825
2	2.755	7	2.555	12	2.185	17	1.73
3	2.735	8	2.49	13	2.1	18	1.635
4	2.7	9	2.425	14	2.01	19	1.54
5	2.66	10	2.35	15	1.915	20	1.445

eigenvalue spectrum and the eigenfunctions obtained from the lattice approximation coincide, with a very good precision, with the well-known analytical results (6), (5), provided we replace the continuous parameter ν by the discrete lattice parameter,

$$\nu_n = \frac{2.9n}{\ln(\kappa_{\max}/\kappa_{\min})}. \tag{95}$$

We view this as a test of our lattice approximation.

For the massive case, the positive eigenvalues are described very well by the same expression with ν_n being replaced by

$$\nu_n^{(M)} = \frac{2.9n}{\ln(\kappa_{\max}/(\kappa_{\min}+M^2))}. \tag{96}$$

The first twenty eigenvalues are given in Table I. The lattice value of the leading intercept differs from its analytical result $\omega_{\text{BFKL}}/\bar{\alpha}_{\text{e.w.}} = 4\ln 2 \approx 2.77$ by 3×10^{-5}, which illustrates a very high precision of the chosen method. The eigenfunctions with positive intercepts can be parametrized as

$$\phi_n^{(\text{approx})}(\kappa) = \frac{\alpha(n)}{\sqrt{\kappa+4}}\sin(\nu_n^{(M)} Ln(\kappa)+\varphi_n),$$
$$Ln(\kappa) \equiv \ln\left(\frac{\sqrt{\kappa+4}+\sqrt{\kappa}}{\sqrt{\kappa+4}-\sqrt{\kappa}}\right), \tag{97}$$

where $\varphi_n = b_\phi \nu_n^{(M)}$ with $b_\phi \approx 1.865$. In the continuum limit we should replace the discrete variable $\nu_n^{(M)}$ by the continuous variable ν. As we can see from Fig. 1, indeed the transition to the continuum spectrum (limit $\kappa_{\max}\to\infty$) is smooth.

C. Corrections proportional to $\sin^2\theta_W$

In this section we will estimate the corrections of the order $\propto s_W^2$ to the leading intercept. A small value of the parameter $(s_W^2)_{\text{phys}} \equiv \sin^2\theta_W = 0.234 \pm 0.0013$ implies that a perturbative expansion should converge rapidly. While application of the perturbation theory for the shift of band in a continuum spectrum is not well defined, in the lattice the spectrum is discrete, so an ordinary perturbation theory is applicable provided first order corrections are smaller than the distance between the neighbor states. In this section we assume this, and show that the corresponding correction to the intercept explicitly vanishes. In the first order of perturbation theory, the shift of the leading intercept is given by

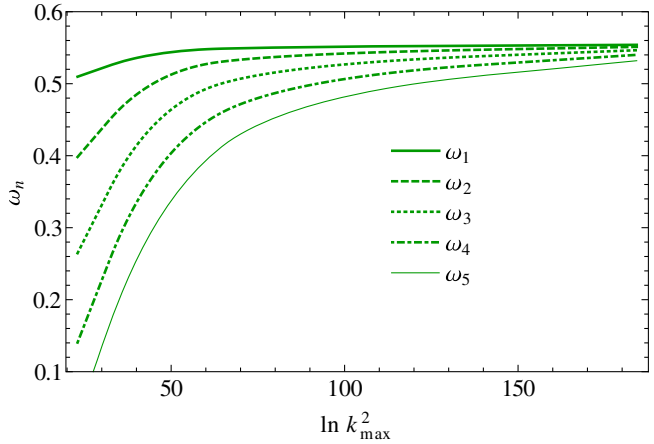

FIG. 1. Dependence of eigenvalues on the ultraviolet cutoff $\kappa_{\max}$. Only the first five eigenvalues are shown; eigenvalues with larger n uniformly fill in the band $\omega \lesssim \omega_0$.

$$\Delta\omega_1 = \frac{\int d\kappa d\kappa' \phi_1(\kappa)\Delta\mathcal{K}(\kappa,\kappa')\phi_1(\kappa')}{\|\phi_1\|^2}, \tag{98}$$

where the kernels $\Delta\mathcal{K}$ were introduced earlier in (51)–(66), and the norm $\|\phi_n\|$ is defined as

$$\|\phi_1\|^2 = \int d\kappa |\phi_1(\kappa)|^2. \tag{99}$$

Using the parametrization of ϕ_1 from (97), we can see that the norm (99) is growing as a function of upper cutoff as $\propto \ln\kappa_{\max}$, which is a manifestation of the fact that we work with wave functions of continuum spectrum. For this reason we should only focus on the large-$\kappa_{\max}$ behavior of the different contributions to numerator. As we can see from (40)–(43), (50), all the contributions to $\Delta\mathcal{K}$ from expansion of masses in kernels ΔK and Regge trajectories $\Delta\omega_c$ have an additional suppression $\mathcal{O}(M^2/k^2)$ and thus lead to finite contributions to the numerator (vanishing contributions to $\Delta\omega_1$) in the limit[6] $\kappa_{\max}\to\infty$. Similarly, all the contributions due to expansion of mass M_Z in propagators do not affect $\Delta\omega_1$.

[6]See Appendix A 2 for a more detailed explanation and numerical estimates.

More complicated is evaluation of the $\mathcal{O}(s_W^2)$ terms which stem from numerators of (9) which do not have any additional power suppression. Approximating all kernels in (40)–(43), (50) with $K_{em}(k,k')$ and using

$$\int d\kappa' K_{em}(\kappa,\kappa')\phi_1(\kappa') \approx (\omega_1 - 2\omega_n(\kappa))\phi_1(\kappa) + \mathcal{O}\left(\frac{M^2}{\kappa}\right), \tag{100}$$

we obtain for the leading contributions to the numerator of (98):

$$\begin{aligned}&\int d\kappa\phi_1(\kappa)\int d\kappa' K_{em}(\kappa,\kappa')\phi_1(\kappa') \\ &= \int d\kappa\phi_1(\kappa)(\omega_1 - 2\omega_n(\kappa))\phi_1(\kappa) \\ &\approx 2\int d\kappa\phi_1^2(\kappa)\omega(\kappa)d\kappa \approx 2\int d\kappa \ln\kappa\phi_n^2(\kappa). \end{aligned} \tag{101}$$

Separately each of these contributions leads to a logarithmically divergent correction to eigenvalue

$$\frac{\int d\kappa d\kappa'\phi_1(\kappa)K_{em}(\kappa,\kappa')\phi_1(\kappa')}{\|\phi_1\|^2} \propto \ln\kappa_{\max} \gg 1. \tag{102}$$

However, in the sum over all components there are strong cancellations of all such contributions. Indeed, as we can see from (40)–(50), such corrections might appear only from $K_{cc,ij}$,[7] which in the large momentum limit has a structure

$$\Delta K_{cc,ij}(\kappa,\kappa') \approx 4s_W^2\eta_{ij}K_{em}(\kappa,\kappa')\left(1 + \mathcal{O}\left(\frac{M^2}{\kappa}\right)\right), \tag{103}$$

where

$$\eta_{Z\gamma} = \eta_{n\gamma} = \eta_{3\gamma} = -\eta_{ZZ} = -\eta_{Zn} = -\eta_{Z3} = 1. \tag{104}$$

After summing all terms in the last line and taking into account the large momentum asymptotic relations (29) and (30) for the components of ϕ_{ij}, we can see that there is a full cancellation of all leading terms. The $\mathcal{O}(\frac{M^2}{\kappa})$-corrections lead to finite contributions to the numerator (vanishing contribution to $\Delta\omega$). As a consequence, the correction (98) decreases as $1/\ln(\kappa_{\max})$ in the infinite lattice limit. This finishes a proof that the $\mathcal{O}(\sin^2\theta_W)$ term vanishes in the $\kappa_{\max}\to\infty$ limit. These cancellations are a mere consequence of the fact that the large momentum limit of the theory with Higgs mechanism is the same as for the pure $SU(2)$ Pomeron.

[7] K_{cccc} also contains K_{em}, but the propagator of the charged field does not contain s_w^2.

D. Corrections proportional to $\sin^4\theta_W$ and the continuum limit

The corrections of the order of $\mathcal{O}(s_W^4)$ are relevant not only for academic interest but also because they allow us to verify that the discrete spectrum perturbation theory is applicable to analysis of discretized eigenvalues in the lattice. There are two sources of such corrections. The corrections which stem from $\mathcal{O}(s_W^4)$-expansion terms in the kernels and propagators can be estimated from (98). From analysis of the coefficients in front of K_{em} in kernel components $K_{cc,ZZ}$, $K_{\gamma Z,cc}$ and $K_{\gamma\gamma,cc}$, we may repeat the line of reasoning of a previous section and demonstrate that large $\mathcal{O}(s_W^4)$-corrections which stem from the numerators of propagators in ZZ, γZ and $\gamma\gamma$ states vanish.

More complicated is the structure of the $\mathcal{O}(s_W^4)$-corrections in the second order of a perturbation theory which are given by

$$\Delta^{(2)}\omega = \sum_{i,i\neq 1}\frac{(\Delta\omega_{1i})^2}{\omega_1 - \omega_i}, \tag{105}$$

where we have introduced a shorthand notation for the transition matrix element

$$\Delta\omega_{1i} = \frac{\int d\kappa d\kappa'\phi_1(\kappa)\Delta K(\kappa,\kappa')\phi_i(\kappa')}{\|\phi_i\|\|\phi_i\|}, \tag{106}$$

and $\|\phi_i\|$ is defined in (99).

Following the analysis of the first order perturbation theory, we derive that $\Delta\omega_{1i}$ behaves as $1/\ln(\kappa_{\max})$ in the infinite lattice limit. The splitting of levels in denominator of (105) for the leading intercept behaves as[8] $\omega_1 - \omega_i \propto 1/\ln^2(\kappa_{\max}/(\kappa_{\min}+1))$ due to $\mathcal{O}(\nu^2)$ behavior of (5) near $\nu = 0$. As a consequence, the ratio (105) is stable in the limit $\kappa_{\max}\to\infty$ and deserves special attention. As shown in Appendix A 2, numerically the ratio is small, which justifies application of perturbative expansion to discretized lattice spectrum. We see two sources of the numerical smallness in each term of (105): the large value of the second derivative $D = |\chi''(\nu)_{\nu=0}| = 28\zeta(3) \approx 33.6$ and the oscillatory behavior of the integrand in the numerator of (106) (which is a manifestation of the orthogonality of ϕ_1 and ϕ_i when $\Delta K \approx$ const).

IV. LATTICE ANALYSIS FOR NONZERO θ_W

In this section we construct a general solution of the Weinberg-Salam model with nonzero θ_W. We demonstrate that the system (13) and (15) can be reduced to a single integral equation (113) for the function ϕ_{cc}. We do not make any assumptions about smallness of Weinberg angle

[8] Note that this estimate is valid only for the leading intercept. For all other eigenvalues $\omega_j - \omega_i \propto 1/\ln(\kappa_{\max}/(\kappa_{\min}+1))$, so the ratio (106) vanishes.

θ_W nor select any restricted kinematics in momentum space. We start our analysis from the observation that the kernel $K_{ij,j'j'}$ in (13) may be factorized into two parts, as

$$K_{ij,j'j'} = g^2 \frac{M_W^2}{2c_W^{2N_Z(i,j,i',j')}} = g^2 \frac{M_W^2}{2c_W^{2N_Z(i,j)} c_W^{2N_Z(i',j')}} \equiv g^2 \frac{M_i^2 M_j^2}{2M_W^2} \frac{1}{c_W^{2N_Z(i',j')}}. \quad (107)$$

We notice that $c_W^{2N_Z(i',j')}$ in the denominator of (107) cancels against similar factors in the numerator of (13), which allows to cast the latter into the form

$$(\omega - N_n(i,j)\omega_n(k))\Phi_{ij}(k) = g^2 \frac{M_i^2 M_j^2}{2M_W^2} \int \frac{d^2k'}{(2\pi)^3} \varphi_\Sigma(k') + \sqrt{2} \int \frac{d^2k'}{(2\pi)^3} \frac{K_{ij,cc}(k,k')\Phi_{cc}(k')}{D(k',M)^2} \quad (108)$$

or

$$\Phi_{ij}(k) = (\omega - N_n(i,j)\omega_n(k))^{-1} \left[g^2 \frac{M_i^2 M_j^2}{2M_W^2} \int \frac{d^2k'}{(2\pi)^3} \varphi_\Sigma(k') + \sqrt{2} \int \frac{d^2k'}{(2\pi)^3} \frac{K_{ij,cc}(k,k')\Phi_{cc}(k')}{D(k',M)^2} \right], \quad (109)$$

where

$$\begin{aligned} \varphi_\Sigma(k) &\equiv \sum_{ij\neq\gamma} (-1)^{N_3(i,j)} \frac{\Phi_{ij}(k)}{D(k,M_i)D(k,M_j)} \\ &= \sum_{ij\neq\gamma} (-1)^{N_3(i,j)} ((\omega - N_n(i,j)\omega_n(k))D(k,M_i)D(k,M_j))^{-1} \\ &\quad \times \left[g^2 \frac{M_i^2 M_j^2}{2M_W^2} \int \frac{d^2k'}{(2\pi)^3} \varphi_\Sigma(k') + \sqrt{2} \int \frac{d^2k'}{(2\pi)^3} \frac{K_{ij,cc}(k,k')\Phi_{cc}(k')}{D(k',M)^2} \right]. \end{aligned} \quad (110)$$

Equation (110) contains, on the rhs, $\varphi_\Sigma(k')$ only as part of the integral $\int d^2k' \varphi_\Sigma(k')$. So we take the integral over k of both sides and solve for $N_\Sigma[\Phi_{cc}] \equiv \int \frac{d^2k}{(2\pi)^3} \varphi_\Sigma$:

$$\begin{aligned} N_\Sigma[\Phi_{cc}] &\equiv \int \frac{d^2k}{(2\pi)^3} \varphi_\Sigma(k) \\ &= \left[\sqrt{2} \int \frac{d^2k}{(2\pi)^3} \int \frac{d^2k'}{(2\pi)^3} \sum_{ij\neq\gamma} \frac{(-1)^{N_3(i,j)} K_{ij,cc}(k,k')\Phi_{cc}(k')}{(\omega - N_n(i,j)\omega_n(k))D(k,M_i)D(k,M_j)D(k',M)^2} \right] \\ &\quad \times \left[1 - g^2 \sum_{ij\neq\gamma} \int \frac{d^2k}{(2\pi)^3} \frac{(-1)^{N_3(i,j)}}{(\omega - N_n(i,j)\omega_n(k))D(k,M_i)D(k,M_j)} \frac{M_i^2 M_j^2}{2M_W^2} \right]^{-1}. \end{aligned} \quad (111)$$

For a given Φ_{cc} from (110) and (111) we can immediately extract $\phi_\Sigma(k)$. Returning to (109) we notice that on the rhs again this factor $N_\Sigma[\phi_{cc}]$ appears, and we can write

$$\Phi_{ij}(k) = (\omega - N_n(i,j)\omega_n(k))^{-1} \left[g^2 \frac{M_i^2 M_j^2}{2M_W^2} N_\Sigma[\Phi_{cc}] + \sqrt{2} \int \frac{d^2k'}{(2\pi)^3} \frac{K_{ij,cc}(k,k')\Phi_{cc}(k')}{D(k',M)^2} \right]. \quad (112)$$

Finally, substituting (112) into (15) and combining with (109) and (110) we arrive at

$$\begin{aligned} (\omega - 2\omega_c(k))\Phi_{cc}(k) &= \int \frac{d^2k'}{(2\pi)^3} \frac{K_{cc,cc}(k,k')\Phi_{cc}(k')}{D(k',M_W)^2} + g^2 \frac{M_W^2\sqrt{2}}{2} N_\Sigma[\Phi_{cc}] \\ &\quad \times \int \frac{d^2k'}{(2\pi)^3} \sum_{ij\neq\gamma} \frac{K_{cc,ij}(k,k')(-1)^{N_3(i,j)}}{(\omega - N_n(i,j)\omega_n(k'))D(k',M_i)D(k',M_j)} \\ &\quad + 2 \int \frac{d^2k'}{(2\pi)^3} \int \frac{d^2k''}{(2\pi)^3} \sum_{ij} \frac{K_{cc,ij}(k,k')(-1)^{N_3(i,j)} c_W^{2N_Z(i,j)} s_W^{2N_\gamma(i,j)} K_{ij,cc}(k',k'')\Phi_{cc}(k'')}{(\omega - N_n(i,j)\omega_n(k'))D(k',M_i)D(k',M_j)D(k'',M_W)^2}. \end{aligned} \quad (113)$$

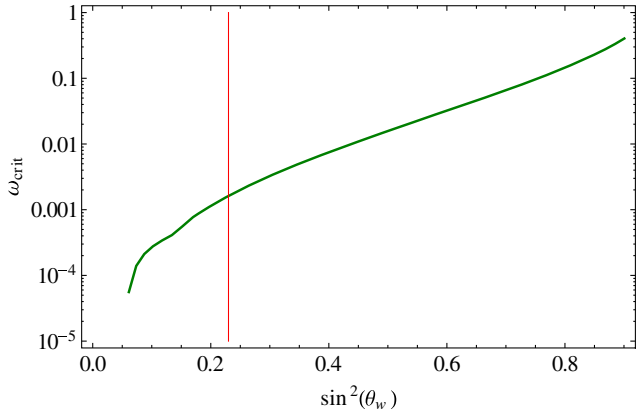

FIG. 2. Behavior of the critical eigenvalue $\omega_{\rm crit}$ which causes a pole in the second line of Eq. (111). The vertical red line stands for the physical value of Weinberg angle θ_W.

Equation (113) represents a linear integral equation for Φ_{cc}. Further simplifications of Eq. (113) are not possible, so we use numerical methods for its analysis.

In Sec. III A we have demonstrated that in the case $\theta_W = 0$, instead of (113), the isospin zero wave function might be found as a solution of a much simpler equation (83). Albeit (113) does not reduce to (83) in the limit $\theta_W = 0$, it is possible to demonstrate that any solution of (83) is also a solution of (113) in this limit (see Appendix A 3 for details). The fact that, in general, the spectrum depends on θ_W can be seen from the second line in Eq. (111): for nonzero θ_w due to incomplete cancellation of contributions of Z and 3 in the denominator appears a term $\sim O(s_W^4)/\omega$. This contribution for sufficiently small positive ω leads to a pole. The position of this pole (ω_0) depends on the value of θ_W, as shown in Fig. 2, and signals that near the pole there could be a sizable sensitivity to θ_W. A dependence on θ_w is also contained in the last line of Eq. (111). It turns out that net dependence on θ_W, for the leading eigenvalue, is negligible. This result can be traced back to the fact that, in the region of large transverse momenta, the equation approaches the BFKL equation.

Equation (113) is not a canonical eigenvalue problem. Instead, ω appears in the denominators in the rhs. In order to solve the equation for ω, we use the following method:

(i) On the rhs of (113) we replace ω everywhere by a fixed parameter[9] $\omega^{(r)}$, thus converting Eq. (113) into an ordinary eigenvalue problem.

(ii) We apply the method of Sec. III B 1 to solve this eigenvalue problem, and find the corresponding eigenvalues $\omega^{(l)} = \omega^{(l)}(\omega^{(r)})$ as functions of the fixed parameter $\omega^{(r)}$.

(iii) We extract the true eigenvalues of Eq. (113) by solving the algebraic equation $\omega^{(l)}(\omega^{(r)}) = \omega^{(r)}$.

[9]The superscripts l and r stand for "left" and "right"-hand side substitutions of ω.

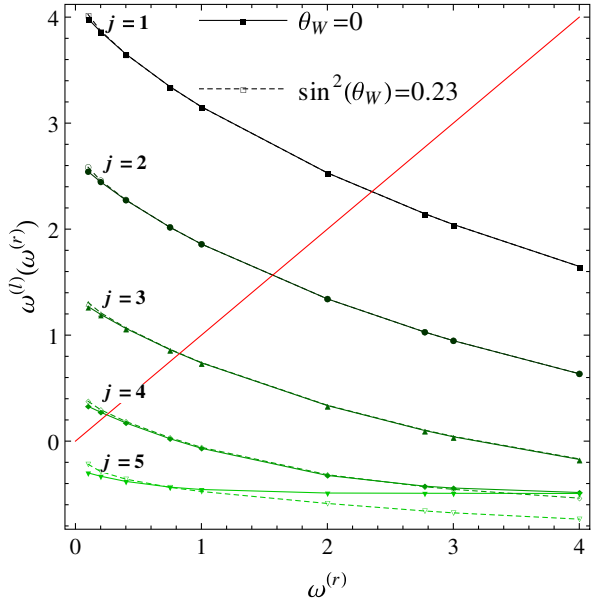

FIG. 3. Root trajectories $\omega^{(l)}(\omega^{(r)})$. Dashed lines correspond to physical mixing angle θ_W. The red line stands for $\omega^{(l)} = \omega^{(r)}$. We use units $\bar{\alpha}_{\rm e.w.} = 1$. For the upper cases $j = 1, 2, 3, 4$ the solid lines ($\theta_W = 0$) and the dashed lines (physical mixing angle) are practically indistinguishable, i.e. they are nearly identical.

Due to the complexity of the equation (113) and to the finite precision of our numerical evaluation, we cannot extend our lattice up to very large $\kappa = \frac{k^2}{m^2} \sim 10^{80}$, as we did in Sec. III B 1. We fix the minimal and maximal values of κ and the number of nodes N as

$$\kappa_{\rm min} = 10^{-10}, \qquad \kappa_{\rm max} = 10^{15}, \qquad N = 4096. \tag{114}$$

Figure 3 illustrates that the root trajectories $\omega^{(l)}(\omega^{(r)})$ are homogeneously decreasing functions of parameter $\omega^{(r)}$, as expected from (113). For this reason, each trajectory $\omega^{(l)}(\omega^{(r)})$ gives rise to only one root ω_j. In agreement with our results of the previous section, for the leading root the effect of a nonzero mixing angle θ_W is negligible. However, this result is not universal, and for $\omega \approx 0$ the dependence is much stronger. Finally, in Table II we give numerical values for positive roots.

Due to the relatively small size of the lattice (114), we obtain only four positive roots, in agreement with what was found in Sec. III B 1 in Fig. 1. We expect that with an increase of the size of the lattice the intercept of the leading pole will grow up to its true value $4\ln 2$, as well as the distance between the neighboring roots will decrease as shown in Fig. 1.

Despite the somewhat low precision of the above estimates, we clearly see from Table II that the first root does not depend on the value of θ_W for any value of θ_W. As it has been discussed, we know the spectrum at $\theta_W = 0$ and we know the first order correction in $\sin^2(\theta_W)$. Therefore,

TABLE II. The positive roots $\omega_j/\bar{\alpha}_{\text{e.w.}}$ of (113) evaluated with lattice parameters (114).

j	$\theta_W = 0$	$\sin^2\theta_W = 0.23$
1	2.335	2.331
2	1.561	1.560
3	0.839	0.845
4	0.245	0.262

we can conclude that for $\theta_W \neq 0$ the spectrum of the electro-weak Pomeron is the same as the spectrum of the massless BFKL equation, with the replacement $\bar{\alpha}_S \to \bar{\alpha}_{\text{e.w.}}$.

V. CONCLUSIONS

In this paper we have analyzed the spectrum of the electroweak BFKL Pomeron, both using perturbative (in θ_W) methods as well as a numerical nonperturbative study on the lattice (for $\theta_W \neq 0$). We found that the leading intercept important for the high energy behavior of the amplitudes depends on θ_W very weakly, and for physical value of θ_W differs from the special case $\theta_w = 0$ by less than 1% (see Table II). However, for subleading intercepts the dependence on θ_w is more pronounced. On the other hand, since we have a continuous spectrum, this dependence is not important for the description of the processes.

The leading order intercept is given by $\Delta_{\text{e.w.}} = \omega_0 \approx \frac{8\alpha_{\text{e.w.}}}{\pi}\ln 2 \approx 0.176$, where $\alpha_{\text{e.w.}}$ is the electroweak fine structure constant. Numerically, this is a small number. However at, for example, $W = \sqrt{s} = 30$ TeV the contribution of the electroweak Pomeron $\propto (s/M_W^2)^{\Delta_{\text{e.w.}}}$, at $W = \sqrt{s} = 30$ TeV gives already an enhancement of the order of $\exp(0.176\ln(W^2/M_W^2)) \approx 8$ which is not small.

On the other hand, in all practical applications the high energy behavior is dominated by the inclusion of the QCD Pomeron, whose intercept is enhanced by a factor $\frac{3}{2}\frac{\alpha_s}{\alpha_{\text{e.w.}}}$ (see Fig. 4). So the real problem is the coexistence and mixing of the QCD Pomeron with the electroweak one. Let us give an example. First, because of the external coupling the contribution of the QCD Pomeron is suppressed by the factor $\alpha_{\text{e.w.}}\bar{\alpha}_S^2$ in comparison to the electroweak Pomeron. Next, for $W = 30$ TeV the ratio of the QCD Pomeron to the electroweak can be estimated as $\alpha_{\text{e.w.}}\bar{\alpha}_S^2 \exp(\bar{\alpha}_S 4\ln 2\ln(W^2/Q^2) - 0.176\ln(W^2/M_W^2))$ where Q is the virtuality of W, Z, γ in the electroweak process. For $Q = 1$ GeV and $\bar{\alpha}_S = 0.2$ we see that the ratio is about 20, showing that the QCD Pomerons win. However, this conclusion may be a bit premature since the intercept of the QCD Pomeron is strongly affected by the QCD next-to-leading order corrections while such QCD corrections do not change the intercept of the electroweak Pomeron. Pure electroweak corrections are not known. Assuming that the QCD corrections diminish the intercept of the QCD Pomeron by a factor of 2 (as it follows from the phenomenology of deep inelastic scattering), we see that the ratio is about 0.1 showing that we might have a window in the energy in which we are able to measure and to investigate the electroweak Pomeron. The energy $W = 30$ TeV perhaps is too large for the real experiment. At a more realistic energy, $W = 3$ TeV, the effect of the electroweak Pomeron is smaller than at $W = 30$ TeV. leading to $\exp(0.176\ln(W^2/M_W^2)) \approx 3.6$. The contribution of the QCD Pomeron is negligibly small. Therefore, this energy might give a reasonable compromise between a realistic experimental possibility and seeing an enhancement due to electroweak Pomeron contribution.

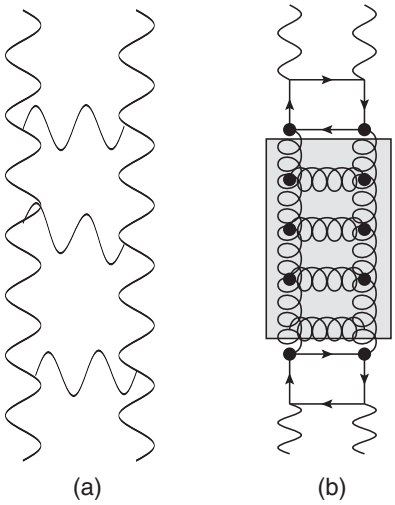

FIG. 4. (a) The contribution of the electroweak Pomeron to an electroweak scattering process. (b) Contribution of the QCD Pomeron to the same electroweak processes. External wavy lines stand for electroweak bosons (Z, W, γ), the grey blob with gluon ladder inside stands for the QCD Pomeron.

We consider our results as an important demonstration that low-energy effects [like symmetry breaking and mixing of $SU(2)$ with $U(1)$ in physical bosons] do not affect the leading intercept describing the high energy behavior. A small value of the intercept also ensures that higher order loop corrections remain small and can be addressed perturbatively.

An interesting future step of our study is the inclusion of the running coupling. It is known from the study of the QCD Pomeron [11] that the running of α_s leads to a discrete spectrum. The two gluon wave function belonging to the leading BFKL eigenvalue is concentrated at smaller momenta, and for this reason we expect a stronger sensitivity to the infrared behavior of the theory. In electroweak theory, this should translate into a stronger sensitivity to a Higgs mechanism and to the value of the mixing angle.

If the electroweak standard model with one Higgs boson remains the correct theory at LHC energies and beyond it may be interesting to extrapolate scattering processes and unitarity constraints up to energies where strong and

electroweak couplings become comparable. At such energies, QCD and the electroweak sector will mix, and unitarization should affect both sectors. Our analysis presented in this paper may provide a starting point for addressing such questions.

ACKNOWLEDGMENTS

We thank Lev Lipatov and our colleagues at UTFSM and at Tel Aviv University for encouraging discussions. One if us (J. B.) wants to thank the theory group of UTFSM for their generous hospitality. This research was partially supported by the BSF Grant No. 2012124, by Proyecto Basal FB 0821 (Chile), Fondecyt (Chile) Grants No. 1140377 and No. 1140842, CONICYT (Chile) Grants No. PIA ACT1406 and No. ACT1413, and MEC-80140070. Powered@NLHPC: This research was partially supported by the supercomputing infrastructure of the NLHPC (ECM-02). Also, we thank Yuri Ivanov for technical support of the USM HPC cluster where part of the evaluations were done.

APPENDIX:

1. Discrete state of the BFKL equation for massive gluon

In [5] we found that in a limit $\theta_W \to 0$ the spectrum of the BFKL with massive boson is continuous and coincides with spectrum of massless QCD. Now we would like to demonstrate that the theory possesses additional discrete levels absent in the massless limit. However, we overlooked in that paper the existence of a new discrete level with the intercept $\omega_{\rm discr} = -\frac{5}{8}\bar{\alpha}_{\rm e.w.}$ and with the eigenfunction given by

$$\phi_{cl}(\kappa) = \frac{1}{1+\kappa}. \tag{A1}$$

Plugging the ansatz (A1) into (89), we may see that the contributions of the first and the third terms in (90) mutually cancel, and the contribution of the second term yields for the eigenvalue $\omega_{\rm discr} = -\frac{5}{8}\bar{\alpha}_{\rm e.w.}$. In a diagrammatic language this solution corresponds to a sum of the diagrams in Fig. 5.

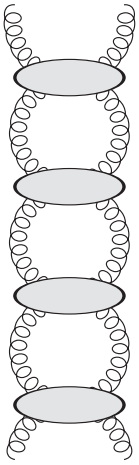

FIG. 5. The diagrams that lead to the discrete level due to contact term interaction.

However, in a general case $\theta_W \neq 0$ we can see that solutions of a form

$$\Phi_{ij} = \frac{c_{ij}}{D(k,M_i)D(k,M_j)}, \tag{A2}$$

$$\Phi_{cc} = \frac{c}{D(k,M)^2} \tag{A3}$$

do not satisfy the eigenvalue equations (13) and (15).

2. Numerical results of $\Delta\omega_1$

In Sec. III C we argued that a correction (98) is suppressed in the limit $\kappa_{\rm max} \to \infty$. In this section we give for the sake of reference corresponding contributions of different components in order to support this claim. We use shorthand notations $\boldsymbol{\Delta\omega_1^{\Delta K}}$ for the $\mathcal{O}(s_W^2)$-corrections to kernels (40)–(43) and (50) and $\boldsymbol{\Delta\omega_1^{\Delta P}}$ due to $\mathcal{O}(s_W^2)$-corrections to propagators. Using an upper cutoff as in Sec. III B 1, we found

$$\boldsymbol{\Delta\omega_1^{\Delta K}} = s_W^2 10^{-4} \times \begin{pmatrix} & ZZ & \tilde{n}\,\tilde{n} & \{Z\tilde{n}\} & 33 & \{Z3\} & \{\tilde{n}3\} & cc \\ ZZ & 1.10 & 0.55 & 1.65 & 0.55 & -1.65 & -1.65 & 0.48 \\ \tilde{n}\,\tilde{n} & 0.55 & 0 & 0.55 & 0 & -0.55 & -0.55 & 0 \\ \{Z\tilde{n}\} & 0.82 & 0.27 & 1.10 & 0.27 & -1.10 & -1.10 & 0.24 \\ 33 & 0.55 & 0 & 0.55 & 0 & -0.55 & -0.55 & 0.24 \\ \{Z3\} & -0.82 & -0.27 & -1.10 & -0.27 & 1.10 & 1.10 & -0.24 \\ \{\tilde{n}3\} & -0.82 & -0.27 & -1.10 & -0.27 & 1.10 & 1.10 & -0.24 \\ cc & 0.48 & 0 & 0.48 & 0 & -0.48 & -0.48 & -24 \end{pmatrix} \tag{A4}$$

and

$$\boldsymbol{\Delta\omega}_{\mathbf{1}}^{\mathbf{\Delta P}} = s_W^2 10^{-4} \times \begin{pmatrix} & ZZ & \tilde{n}\,\tilde{n} & \{Z\tilde{n}\} & 33 & \{Z3\} & \{\tilde{n}3\} & cc \\ ZZ & -3.16 & 0 & -2.58 & 0 & 2.58 & 0 & 0 \\ \tilde{n}\,\tilde{n} & 0.82 & 0.27 & 1.10 & 0.27 & -1.10 & -1.10 & 0.24 \\ \{Z\tilde{n}\} & 0.82 & 0.27 & 1.10 & 0.27 & -1.10 & -1.10 & 0.24 \\ 33 & 0.82 & 0.27 & 1.10 & 0.27 & -1.10 & -1.10 & 0.24 \\ \{Z3\} & 0.82 & 0.27 & 1.10 & 0.27 & -1.10 & -1.10 & 0.24 \\ \{\tilde{n}3\} & 0.82 & 0.27 & 1.10 & 0.27 & -1.10 & -1.10 & 0.24 \\ cc & L-8.90 & 0 & 0.89-L & 0 & L-0.89 & 0 & 0 \end{pmatrix} \tag{A5}$$

where $L = -0.53 \times 10^4$. We can see that, indeed, all corrections except those $\sim L$ are small and vanish in the limit $\kappa_{\max} \to \infty$. The components $\sim L$ vanish in a full sum, which finishes the proof that the corrections are small.

3. Proof that (113) includes (83) for $\theta_W = 0$

In this section we demonstrate explicitly that for the case $\theta_W = 0$ any solution of Eq. (83) does satisfy Eq. (113). Indeed, we may rewrite (83) as

$$\int d^2k' K_{em}(k,k') \frac{\Phi_{cc}(k')}{D^2(k')} = -g^2 \frac{5M_W^2}{8} \int d^2k' \frac{\Phi_{cc}(k')}{D^2(k')} + \frac{(\omega - 2\omega(k))}{4} \Phi_{cc}(k). \tag{A6}$$

Since in the limit $\theta_W = 0$ the kernels $K_{ij,cc}$ and $K_{cc,cc}$, up to a constant, are proportional to $K_{em}(k,k')$,

$$K_{cc,cc}(k,k') = -g^2 M_W^2 + 2K_{em}(k,k') \tag{A7}$$

$$K_{cc,nn}(k,k') = -\frac{3g^2 M_W^2}{2} + 2K_{em}(k,k'), \tag{A8}$$

we can use (A6) to evaluate explicitly the convolutions. Equation (113) in the limit $\theta_W = 0$ is given by

$$\begin{aligned}(\omega - 2\omega_n(k)) D(k,M_W)^2 \phi_{cc}(k) = {} & \int d^2k' [-M_W^2 + 2K_{em}(k,k')] \frac{\Phi_{cc}(k')}{D^2(k')} + \frac{M_W^2}{2} \frac{f(k) \int d^2k' f(k') \Phi_{cc}(k')/D^2(k')}{1 - \frac{M_W^2}{2} \int \frac{d^2k}{(\omega - 2\omega_n(k)) D^2(k)}} \\ & + 2 \int d^2k' \int d^2k'' \frac{K_{cc,nn}(k,k') K_{nn,cc}(k',k'')}{(\omega - 2\omega_n(k')) D^2(k')} \frac{\Phi_{cc}(k'')}{D^2(k'')},\end{aligned} \tag{A9}$$

where

$$f(k) = \sqrt{2} \int d^2k' \frac{K_{cc,nn}(k,k')}{(\omega - 2\omega_n(k')) D^2(k')}. \tag{A10}$$

A straightforward application of (A6) after some algebra yields

$$\int d^2k' f(k') \frac{\Phi_{cc}(k')}{D^2(k')} = \frac{\sqrt{2}}{2} \int d^2k' \frac{\Phi_{cc}(k')}{D^2(k')} \left[1 - \frac{M_W^2}{2} \int \frac{d^2k}{(\omega - 2\omega_n(k)) D^2(k)} \right], \tag{A11}$$

$$\frac{M_W^2}{2} \frac{f(k) \int d^2k' f(k') \Phi_{cc}(k')/D^2(k')}{1 - \frac{M_W^2}{2} \int \frac{d^2k}{(\omega - 2\omega_n(k)) D(k) D(k)}} = \frac{M_W^2}{2} \int d^2k'' \frac{\Phi_{cc}(k'')}{D^2(k'')} \int d^2k' \frac{[-\frac{3M_W^2}{2} + 2K_{em}(k,k')]}{(\omega - 2\omega_n(k')) D^2(k')}, \tag{A12}$$

$$2\int d^2k'\int d^2k''\frac{K_{cc,nn}(k,k')K_{nn,cc}(k',k'')}{(\omega-2\omega_n(k'))D(k')D(k')}\frac{\Phi_{cc}(k'')}{D^2(k'')}=-g^2\frac{M_W^2}{4}\int d^2k'\frac{\Phi_{cc}(k')}{D^2(k')}+\frac{(\omega-2\omega_n(k))}{2}\Phi_{cc}(k)$$
$$-g^2\frac{M_W^2}{2}\int d^2k'\frac{[-\frac{3M_W^2}{2}+2K_{em}(k,k')]}{(\omega-2\omega_n(k'))D^2(k')}$$
$$=\int d^2k''\frac{\Phi_{cc}(k'')}{D^2(k'')}, \tag{A13}$$

and

$$\int d^2k'K_{cc,cc}(k,k')\frac{\Phi_{cc}(k')}{D^2(k')}=\left[\frac{(\omega-2\omega_n(k))\Phi_{cc}(k)}{2}+g^2\frac{M_W^2}{4}\int d^2k''\frac{\Phi_{cc}(k'')}{D^2(k'')}\right]. \tag{A14}$$

After summation of (A11)–(A14) we recover the lhs of (A9).

4. Large transverse momenta

In this Appendix we show how Eq. (113) has the same solution as the BFKL equation at large values of $\kappa > M_Z^2$, which we have discussed in Sec. III [see Eqs. [9] and (28)]. For large κ we can rewrite functions Φ_{ij} and Φ_{cc} of Sec. IV in the form

$$\Phi_{ij}(\kappa)\ \xrightarrow{\kappa\gg M_Z^2}\ D(\kappa,M_i)\phi_W(\kappa)=\kappa\kappa^{-\frac{1}{2}+i\nu},$$
$$\Phi_{cc}(\kappa)\ \xrightarrow{\kappa\gg M_W^2}\ D(\kappa,M_W)\phi_W(\kappa)=\frac{1}{\kappa}\kappa^{-\frac{1}{2}+i\nu}, \tag{A15}$$

where $\phi_W(\kappa)$ is the eigenfunction of the BFKL equation [see Eq. [9]]. In Eq. (A15) we first calculate the last term of Eq. (113):

$$2\int\frac{d^2k'}{(2\pi)^3}\int\frac{d^2k''}{(2\pi)^3}\sum_{ij}\frac{K_{cc,ij}(k,k')(-1)^{N_3(i,j)}c_W^{2N_Z(i,j)}s_W^{2N_\gamma(i,j)}K_{ij,cc}(k',k'')\Phi_{cc}(k'')}{(\omega-N_n(i,j)\omega_n(k'))D(k',M_i)D(k',M_j)D^2(k'',M_W)}. \tag{A16}$$

First, in the sum over i, j we consider the terms with $i=j=n$, which after substituting Eq. (A15) takes the form

$$2\int\frac{d^2k'}{(2\pi)^3}\int\frac{d^2k''}{(2\pi)^3}\frac{K_{cc,nn}(k,k')K_{nn,cc}(k',k'')\phi_W}{(\omega-2\omega_n(k'))D(k',M_W)}$$
$$=2\int\frac{d^2k'}{(2\pi)^3}\int\frac{d^2k''}{(2\pi)^3}\frac{K_{cc,nn}(k,k')(\frac{1}{2}(\omega-2\omega_n(k'))\phi_W(k')-\frac{3}{2}\phi_W(k'')/k''^2)}{(\omega-2\omega_n(k'))D^2(k',M_W)}$$
$$\xrightarrow{k,k',k''\gg M_W}\int\frac{d^2k'}{(2\pi)^3}\frac{K_{cc,nn}(k,k')}{D(k',M_W)}\phi_W(k')\ \xrightarrow{k,k''\gg M_W}\ 2\int\frac{d^2k'}{(2\pi)^3}\frac{K_{em}(k,k')}{D(k',M_W)}\phi_W(k'). \tag{A17}$$

In the second line of Eq. (A17) we use the explicit form of the kernel $K_{nn,cc}(k',k'')$ [see Eq. (19)] while in the last line we neglect the terms that are of the order of $1/k^2$ at large k in comparison $\phi_W(k)$. Note that this term is the same as the first term in Eq. (113). Replacing $K_{cc,ij}(k,k')$ and $K_{ij,cc}(k',k'')$ by $2K_{em}(k,k')$ and $2K_{em}(k',k'')$, respectively, at large k, k' and k'' we can see that the sum over n, j with $j=Z,3,\gamma$ can be reduced to

$$8\int\frac{d^2k'}{(2\pi)^3}\int\frac{d^2k''}{(2\pi)^3}\frac{K_{em}(k,k')K_{em}(k',k'')\phi_{cc}(k'')}{(\omega-\omega_n(k'))k'^4}\underbrace{\{c_W^2-1+s_W^2\}}_{=0}. \tag{A18}$$

Summation over i, j $i=Z,3,\gamma$ and $j=Z,3,\gamma$ reduces to the replacement $\omega-\omega_n(k')\to\omega$ and $\{\cdots\}\to\{c_W^4+1+s_W^4+2c_W^2s_W^2-2c_W^2-2s_W^2\}=0$, in Eq. (A18). Therefore, the only term which contributes at large momenta is the term with $ij=nn$, and Eq. (113) reduces to the BFKL equation [see Eq. [9]] since the second term in Eq. (113) vanishes in this kinematic region. It is instructive to note that we have proven the equivalence of Eqs. (113) and [9] without assuming that $|\kappa-\kappa'|\gg M_W^2$.

[1] J. Bartels, L. N. Lipatov, and K. Peters, Nucl. Phys. **B772**, 103 (2007).
[2] E. A. Kuraev, L. N. Lipatov, and V. S. Fadin, Sov. Phys. JETP **44**, 443 (1976).
[3] Y. Y. Balitsky and L. N. Lipatov, Sov. J. Nucl. Phys. **28**, 822 (1978).
[4] G. Chachamis and K. Peters, Phys. Lett. B **580**, 169 (2004).
[5] E. Levin, L. Lipatov, and M. Siddikov, Phys. Rev. D **89**, 074002 (2014).
[6] E. Levin, L. Lipatov, and M. Siddikov, Eur. Phys. J. C **75**, 558 (2015).
[7] K. A. Olive *et al.* (Particle Data Group Collaboration), Chin. Phys. C **38**, 090001 (2014).
[8] Yuri V. Kovchegov and Eugene Levin, Quantum chromodynamics at high energies, *Cambridge Monographs on Particle Physics, Nuclear Physics and Cosmology* (Cambridge University Press, Cambridge, 2012).
[9] E. A. Kuraev, L. N. Lipatov, and F. S. Fadin, Sov. Phys. JETP **45**, 199 (1977); Ya. Ya. Balitsky and L. N. Lipatov, Sov. J. Nucl. Phys. **28**, 822 (1978).
[10] G. V. Frolov, V. N. Gribov, and L. N. Lipatov, Phys. Lett. B **31**, 34 (1970).
[11] L. N. Lipatov, Phys. Rep. **286**, 131 (1997); Zh. Eksp. Teor. Fiz. **90**, 1536 (1986) [Sov. Phys. JETP **63**, 904 (1986)].
[12] L. N. Lipatov, Phys. Rep. **286**, 131 (1997); Zh. Eksp. Teor. Fiz. **90**, 1536 (1986) [Sov. Phys. JETP **63**, 904 (1986)].
[13] I. Gradstein and I. Ryzhik, *Table of Integrals, Series, and Products*, 5th ed. (Academic Press, London, 1994).
[14] V. S. Fadin, E. A. Kuraev, and L. N. Lipatov, Phys. Lett. B **60**, 50 (1975); Sov. Phys. JETP **44**, 443 (1976); **45**, 99 (1977).